

Mutual attraction of laser beams in plasmas: braided light

C. Ren, R. G. Hemker, R. A. Fonseca*, B. J. Duda, and W. B. Mori

Department of Physics & Astronomy, University of California, Los Angeles, CA 90095-1547

(June 7, 2000)

Using a variational method, we show that an effective attractive force exists between two Gaussian laser beams in a plasma because of a mutual coupling from relativistic mass corrections. The effective force can be generalized to other nonlinearities. This force can cause two laser beams to spiral around each other with a rotation period that is proportional to the Rayleigh length. These orbits are stable if the ratio of the orbit diameter to the laser spot size $d_0/W_0 \leq \sqrt{2}$. Three dimensional particle-in-cell simulations are presented which confirm the mutual attraction.

According to Maxwell's equations, light beams do not interact in vacuum. However, in a nonlinear medium there is a self-interaction, as is clear from the well known self-focusing effect [1]. This leads to an obvious question, is there a mutual interaction between two (or more) light beams in a nonlinear medium? There has been much recent research, both theoretical and experimental, on the interaction between two optical solitons in nonlinear optical media such as optical fibers and photorefractive materials [2]. This work is geared towards applications in optical communications where the laser power and intensities are low. A plasma is another nonlinear medium [3] and it is the only type applicable for high-intensity lasers or other intense radiation sources such as in gamma ray bursters [4]. Furthermore, understanding the mutual interaction between individual light beams is a critical first step towards understanding the interaction of individual filaments of a larger beam [5] or between individual speckles in a random phase plate beam [6].

In this Letter we investigate the mutual interaction between two Gaussian laser pulses in plasmas. During the last few years much effort has been devoted towards understanding the evolution of only one Gaussian pulse in an underdense plasma [3,7,8]. This has proven to be a challenging problem because of the complication in including both the relativistic nonlinearity which leads to self-focusing and self-phase modulation and the coupling to the plasma wave wake which leads to Raman forward scattering processes such as spot-size self-modulation and hosing. Therefore, to make analytical progress we examine a model problem in which the only nonlinearity is that from relativistic mass corrections. We use a variational principle approach [8–10] to obtain coupled equations for the spot sizes and beam centroids of each pulse. These equations demonstrate that there is mutual attractive force between the beams and that this force leads to stable spiraling solutions. We then use the fully explicit and fully three-dimensional particle-in-cell (PIC) code OSIRIS [11] to verify the predictions and to see the importance of other nonlinearities, most notably the wake from Raman forward scattering type instabilities and the energy loss into trapped electrons. The simula-

tions show that the full nonlinearity causes the beams to actually form a braided pattern.

We emphasize that this work differs from previous work on mutual interactions. Here, we examine the attraction between two distinct Gaussian beams and the mutual evolution of each beam's spot size. In past work the modifications to the linear growth rate of one wave by the presence of another wave [12] or the evolution of the total spot size of partially [13] or individual spot sizes of totally [14] overlapping beams were studied. We also emphasize that the mutual interaction we are studying has nothing to do with self-generated magnetic fields. In fact this work offers an alternative explanation for the coalescing of filaments as observed in reference [15].

To demonstrate mutual attraction, we begin with the nonlinear Schrodinger equation with a nonlinearity arising solely from the lowest order relativistic mass corrections

$$(2ik_0 \frac{\partial}{\partial \tau} + \nabla_{\perp}^2 - k_p^2) \vec{a} = -\frac{k_p^2}{4} |a|^2 \vec{a}, \quad (1)$$

where \vec{a} is the envelope of a vector potential with frequency ω_0 , $e\vec{A}/mc^2 = \vec{a}e^{-ik_0c(t-z/c)}/2 + c.c$ and we use the speed of light frame variables ($\tau \equiv z$, $\psi \equiv t - z/c$). We define $k_p^2 \equiv 4\pi ne^2/mc^2$ with n the plasma density and e , m , c , and k_0 are the electron charge, electron mass, speed of light, and laser wave vector, respectively. Keeping only the cubic nonlinear term admits collapsing self-focusing solutions, which in reality can be prevented by including higher order nonlinear terms. In the supporting simulations to be presented here, the spot sizes do not collapse much.

We are interested in how two distinct Gaussian beams interact with each other. We therefore decompose the envelope into two amplitudes and, to isolate certain effects, we assume the two amplitudes are orthogonally polarized, $\vec{a} = \hat{x}_1 a_1 + \hat{x}_2 a_2$ where $(\hat{x}_1, \hat{x}_2) = (\hat{x}, \hat{y})$. Substituting the expression for \vec{a} into Eq.1 gives the following two coupled nonlinear Schrodinger equations:

$$\begin{cases} (2ik_0 \frac{\partial}{\partial \tau} + \nabla_{\perp}^2 - k_p^2) a_1 = -\frac{k_p^2}{4} (|a_1|^2 + |a_2|^2) a_1, \\ (2ik_0 \frac{\partial}{\partial \tau} + \nabla_{\perp}^2 - k_p^2) a_2 = -\frac{k_p^2}{4} (|a_1|^2 + |a_2|^2) a_2. \end{cases} \quad (2)$$

Note that because we have assumed that the two lasers are orthogonally polarized the nonlinearity is always $|a_1|^2 + |a_2|^2$ and no cross terms are present. Furthermore, this generic system of equations can be used to model many other problems in plasma physics and nonlinear optics, with the only difference being the nonlinear coefficients and the normalization for the vector potential. As a result the analysis which follows might have broad applicability and implications.

Obtaining exact solutions to Eq.2 is not possible. However, approximate and parameterized solutions can be obtained using variational principle methods [8–10]. The idea is to first find a Lagrangian density where the Euler-Lagrange equations which result from minimizing the action, $\int_{-\infty}^{\infty} d\tau dx dy \mathcal{L}$, reproduce Eq.2. Such a Lagrangian density is

$$\mathcal{L} = \sum_{j=1,2} [ik_0(a_j \frac{\partial a_j^*}{\partial \tau} - a_j^* \frac{\partial a_j}{\partial \tau}) + \nabla_{\perp} a_j^* \cdot \nabla_{\perp} a_j - k_p^2 (\frac{a_j^2 a_j^{*2}}{8} - a_j a_j^*)] + \mathcal{L}_{\text{int}}, \quad (3)$$

where the coupling term [13] is $\mathcal{L}_{\text{int}} = -k_p^2 a_1 a_1^* a_2 a_2^*$. The variations to a_j and a_j^* are treated independently.

Next, we choose a trial function for each beam. For each beam we use Gaussian trial functions of the form,

$$a_j = A_j e^{-i\phi_j} e^{-i[k_{xj}(x-X_{cj}) + k_{yj}(y-Y_{cj})]} \times e^{[(x-X_{cj})^2 + (y-Y_{cj})^2](ik_0/2R_j - 1/W_j^2)}, \quad j = 1, 2. \quad (4)$$

Here, the amplitude A_j , phase ϕ_j , center (X_{cj}, Y_{cj}) , perpendicular momentum (k_{xj}, k_{yj}) , radius of curvature R_j and spot size W_j are all real and functions of τ . Substituting these trial functions into Eq. 3 and integrating the Lagrangian density over the xy -plane, we obtain a reduced Lagrangian density,

$$\begin{aligned} L &\equiv \frac{2}{\pi} \int_{-\infty}^{\infty} dx \int_{-\infty}^{\infty} dy \mathcal{L} \\ &= \sum_{j=1,2} \left\{ -\frac{k_0 A_j^2 W_j^2}{4} \left[8 \frac{d\phi_j}{d\tau} + \frac{2k_0 W_j^2}{R_j^2} \frac{dR_j}{d\tau} - 8(k_{xj} \frac{dX_{cj}}{d\tau} \right. \right. \\ &\quad \left. \left. + k_{yj} \frac{dY_{cj}}{d\tau}) \right] + \frac{A_j^2}{4} \left[\frac{2k_0^2 W_j^4}{R_j^2} + 8 + 4W_j^2 (k_{xj}^2 + k_{yj}^2) \right] \right. \\ &\quad \left. + k_p^2 W_j^2 \left(A_j^2 - \frac{A_j^4}{16} \right) \right. \\ &\quad \left. - \frac{k_p^2}{4} A_1^2 A_2^2 \frac{W_1^2 W_2^2}{W_1^2 + W_2^2} e^{-2d^2/(W_1^2 + W_2^2)} \right\}. \quad (5) \end{aligned}$$

and hence a reduced action $\int_{-\infty}^{\infty} d\tau L$. Here d is the distance between the centers of the two beams, $d^2 \equiv (X_{c1} - X_{c2})^2 + (Y_{c1} - Y_{c2})^2$. Assuming the best approximate solution occurs when the reduced action is minimized with respect to variations of the trial function parameters

leads to the Euler-Lagrange equations for the reduced Lagrangian density of Eq. 5: $\partial L / \partial \beta - (d/d\tau) \partial L / \partial \dot{\beta} = 0$, where β is a parameter. The resulting equations provide envelope equations for the evolution of the beam parameters. Varying ϕ_j leads to power conservation,

$$\frac{d}{d\tau} (A_j^2 W_j^2) = 0. \quad (6)$$

This prompts us to replace the variables A_j by new variables $P_j \equiv A_j^2 W_j^2$, which are constants. Now varying R_j relates R_j and $dW_j/d\tau$,

$$\frac{W_j}{R_j} = \frac{dW_j}{d\tau}. \quad (7)$$

Varying W_j and using Eq. 7 gives equations for the evolution of each spot size,

$$\begin{aligned} \frac{d^2 W_j}{d\tau^2} + \frac{4}{k_0^2 W_j^3} \left(\frac{P_j k_p^2}{32} - 1 \right) \\ = \frac{k_p^2}{2k_0^2} \frac{P_1 P_2}{(W_1^2 + W_2^2)^2} \frac{W_j}{P_j} e^{-2d^2/(W_1^2 + W_2^2)} \left[-1 + \frac{2d^2}{W_1^2 + W_2^2} \right]. \quad (8) \end{aligned}$$

If the mutual coupling term on the right side is neglected, then Eq.8 reduces to the well known equation for a single beam [1] where $P_j k_p^2 / 32 = P_j / P_c$ and $P_c \approx 17 \omega_0^2 / \omega_p^2 \text{GW}$.

The motion of the beam centroids can be obtained from varying (k_{xj}, k_{yj}) and (X_{cj}, Y_{cj}) . Varying k_{yj} relates k_{yj} and Y_{cj} ,

$$k_{yj} + k_0 \frac{dY_{cj}}{d\tau} = 0, \quad (9)$$

while varying Y_{c1} and Y_{c2} and using Eq. 9 leads to

$$\begin{cases} P_1 \frac{d^2 Y_{c1}}{d\tau^2} = -\frac{k_p^2}{2k_0^2} P_1 P_2 \frac{Y_{c1} - Y_{c2}}{(W_1^2 + W_2^2)^2} e^{-2d^2/(W_1^2 + W_2^2)}, \\ P_2 \frac{d^2 Y_{c2}}{d\tau^2} = \frac{k_p^2}{2k_0^2} P_1 P_2 \frac{Y_{c1} - Y_{c2}}{(W_1^2 + W_2^2)^2} e^{-2d^2/(W_1^2 + W_2^2)}. \end{cases} \quad (10)$$

Similar equations hold in the x -direction. Equations 10 show that the beam centroids move like point particles with a mass proportional to their power. The force is always attractive with an effective exponential potential $V = -(k_p^2 / 4k_0^2) P_1 P_2 / (W_1^2 + W_2^2) \exp[-2d^2 / (W_1^2 + W_2^2)]$. In terms of the centroid motions, momentum conservation in each direction is readily derived from Eqs. 10, e.g., $P_1 \dot{Y}_{c1} + P_2 \dot{Y}_{c2} = \text{const}$. Since the force is central in the xy -plane, the angular momentum of the centroids in the \hat{z} -direction is also conserved [10], i.e., $L \equiv \sum_{j=1,2} P_j (X_{cj} \dot{Y}_{cj} - Y_{cj} \dot{X}_{cj}) = \text{const}$. In general, the force also depends on beam spot sizes, whose evolution is described by Eq. 8.

We consider two simple types of solutions to Eqs. 8 and 10. One possibility is that the two beams spiral around each other. To find simple spiraling solutions, we consider two initially identical beams with initial separation d_0 , $W_{1\text{init}} = W_{2\text{init}} = W_0$ and $P_1 = P_2 = P$. According to Eq.8, the spot sizes remain unchanged,

$d^2W_j/d\tau^2 = 0$, when the power in each beam satisfies $P = P_c e^\alpha / (e^\alpha + 1 - \alpha)$, where $\alpha \equiv (d_0/W_0)^2$. The equations of motion become (from Eqs. 10 and analogous equations in the x -direction)

$$\begin{cases} \frac{d^2\Delta Y_c}{d\tau^2} = -\frac{k_p^2 P}{4k_0^2 W^4} \Delta Y_c e^{-d^2/W^2}, \\ \frac{d^2\Delta X_c}{d\tau^2} = -\frac{k_p^2 P}{4k_0^2 W^4} \Delta X_c e^{-d^2/W^2}, \end{cases} \quad (11)$$

where $\Delta X_c = X_{c1} - X_{c2}$, $\Delta Y_c = Y_{c1} - Y_{c2}$ and $d^2 = (\Delta X_c)^2 + (\Delta Y_c)^2$. There exists a spiraling solution with $\Delta X_c = d_0 \cos \Omega\tau$ and $\Delta Y_c = d_0 \sin \Omega\tau$. The spiraling frequency is proportional to the inverse vacuum Rayleigh length $\tau_R \equiv k_0 W_0^2/2$: $\Omega = \sqrt{2/(e^\alpha + 1 - \alpha)}(\tau_R)^{-1}$. As the beam separation increases, the spiraling period increases exponentially.

To analyze the stability of these spiraling orbits, we perturb the solution as $W = W_0 + \delta W$, $\Delta X_c = (d_0 + \delta d) \cos(\Omega\tau + \delta\phi)$ and $\Delta Y_c = (d_0 + \delta d) \sin(\Omega\tau + \delta\phi)$. Assuming the perturbations evolve as $e^{\gamma\tau}$, we find the growth rate $(\gamma/\Omega)^2 = \alpha^2 - 4$. Therefore the orbits are stable when $d_0 < \sqrt{2}W_0$. Notice that the required power reaches the maximum, $P = P_c/(1 - e^{-2})$, when $d_0 = \sqrt{2}W_0$. Therefore, depending on the perturbation, the two beams in the unstable configuration would either spiral out to infinity or spiral in to a stable configuration which has the same required power.

Another type of solution occurs when the system has no initial angular momentum. Assume that the two beams enter the plasma parallel to each other with $\Delta X_c = 0$, they will oscillate in the y -direction according to Eq. 11, although the oscillation is also coupled to the spot size evolution of Eq. 8. If the spot size change is neglected and $\alpha \ll 1$, then Eq. 11 becomes the well-known Duffing equation for a nonlinear oscillator with a linear frequency of $\sqrt{2P/P_c}\tau_R^{-1}$.

The above theoretical analysis clearly demonstrates that a mutual attraction exists. However, the theory neglects Raman scattering type instabilities and kinetic effects [16] and assumes that the beams remain Gaussian. To demonstrate that such attraction still exists when the full nonlinearities are present and to see the accuracy of the above predictions, we compare the above analysis with 3D fully explicit PIC simulations using a new, object-oriented, fully parallelized code OSIRIS [11]. A typical simulation follows 17 million electrons on a $300 \times 120 \times 120$ grid with a fixed charge neutralizing background of ions for 20,000 time steps. The physical dimensions are $10 c/\omega_p \times 36 c/\omega_p \times 36 c/\omega_p$ and the plasma density is chosen such that $k_0/k_p = 10$. Therefore, the simulation box corresponds to about 16 laser wavelengths (λ_0) in the axial direction and $6.4W_0$ in the transverse directions and the grid resolution is 19 cells/ λ_0 (axial) and 19 cells/ W_0 (transverse).

We are interested in studying the spiraling behavior so the power in each beam is chosen to satisfy the sta-

tionary spot size requirement and the two beams are orthogonally polarized. Furthermore, the theory assumes a weakly relativistic intensity so we choose a normalized vector potential amplitude for each beam $A_j \leq 1$, which corresponds to a normalized electric field for each beam of $E_j = (k_0/k_p)A_j \approx 10$. For smaller values of A and a matched beam, the spot sizes would be too large for the computational grid. The lasers are initialized in the vacuum, using the envelope in Eq. 4. The simulation window moves with a velocity c so that longer propagation distances can be efficiently modeled.

The physical parameters of these simulations can easily be achieved by current laser technology. For a laser wavelength of $1\mu m$, the parameters correspond to a plasma density of $1.1 \times 10^{19} \text{ cm}^{-3}$, and a laser power of 1.1 TW and a spot size of $9\mu m$ for each beam.

In Fig. 1 we plot a time sequence of iso-surfaces of the E -field squared and the calculated centroids ($\vec{X}_c \equiv \int d\vec{x}_\perp \vec{x}_\perp |\vec{E}|^2$) for each laser beam from a simulation where the initial beam separation is $\alpha = 1$ in the y -direction ($Y_{c1} = -Y_{c2} = W_0/2$) and the initial momentum is $-k_{x1} = k_{x2} = 0.015k_0$ and $k_{y1} = k_{y2} = 0$. Therefore the initial angular momentum is Ωd_0 . Since the laser group velocity in the plasma is less than c , the laser pulses slip out of the window. The laser profile rises in $1k_p^{-1}$, is flat for $70k_p^{-1}$ and falls in $10k_p^{-1}$.

The beam's spiraling is clearly shown. The heads of the beams (at the right side of the frames) rotate 180 degrees after $540 \omega_p^{-1}$ (Fig. 1(d)), in agreement with the theoretical prediction of $586 \omega_p^{-1}$. However, the beam tails rotate faster than the heads and the two beams become braided (Fig. 1(c)). We believe this is due to the wake produced by the fast rise of the beams. The wake gives additional focusing to the beam tails. The smaller spot sizes in the tail also lead to a stronger attractive force, which brings the tails closer. As they get closer, the tails rotates faster due to the conservation of angular momentum. We have done runs with longer laser rise times and therefore a weaker wake. As expected, the tails rotate more slowly in this case.

The analogy between laser beam centers and point masses are further verified in cases when the two lasers are not supposed to form a closed orbit. In Figs. 2(a) to (c) a case is plotted where the two beam centers have no initial momentum ($-k_{x1} = k_{x2} = k_{y1} = k_{y2} = 0$). The two beam centroids move toward each other along a straight line and eventually they pass through each other. The oscillation frequency is once again not uniform across the pulse length due to the wake. Figs. 2(a) and (b) show that the wavelength of this variation is approximately one plasma wavelength $2\pi c/\omega_p$. The measured oscillation frequency for the middle part of the pulse agrees with the theoretical prediction. In Fig. 2(d) a case is plotted where the initial angular momentum, $L = 1.7\Omega d_0$, is greater than what is required for a closed orbit. There-

fore as expected, the two beam centers escape away from each other. In these two cases, the initial beam separation is still $\alpha = 1$ and the initial configurations are identical to Fig. 1(a). We have also done spiraling cases where $\alpha > 2$, where the orbit does become unstable and the two beams spiral away from each other.

In conclusion, we have shown analytically that nonlinearities can lead to a mutual attraction between lasers in plasmas. This attraction has been verified in fully explicit PIC simulations which include *all* the nonlinearities. The simulations show that the attraction coupled with the wake lead to braided light; therefore, including the wake in the analysis is an important area for future research. Other issues for future research include the loss of angular momentum when parts of the beam radiate away [5] and the interaction of more than two beams and speckles, using the binary potential developed here. For example, a system of two lasers is integrable while for more than two, the system could be chaotic.

We acknowledge useful conversations with Drs. J. M. Dawson, L. O. Silva, C. Joshi, T. Katsouleas and T. W. Johnston. This work is supported by DOE under Contract Nos. DE-FG03-98DP00211 and DE-FG03-92ER40727, by NSF under Grant No. DMS 9722121 and by the ILSA at LLNL under contract No. W-7405-ENG-48. RAF acknowledges the financial support of Gulbenkian Foundation and FCT (Portugal).

[1] E. Esarey *et al.*, IEEE Journal of Quantum Electronics **33**, 1879 (1997) and the references therein.
[2] G. I. Stegeman and M. Segev, Science **286**, 1518 (1999) and the references therein.
[3] W. B. Mori, IEEE Journal of Quantum Electronics **33**, 1942 (1997) and the references therein.
[4] T. Piran, Phys. Rept. **314**, 575 (1999).
[5] F. Vidal and T. W. Johnston, Phys. Rev. Lett. **77** 1282 (1996).
[6] J. Lindl, Physics of Plasmas **2**, 3933 (1995) and the references therein.
[7] T. M. Antonsen, Jr. and P. Mora, Phys. Rev. Lett. **69**, 2204 (1992); E. Esarey *et al.*, Phys. Rev. Lett. **72**, 2887 (1994); G. Shvets and J. S. Wurtele, Phys. Rev. Lett. **73**, 3540 (1994); P. Sprangle, *et al.*, Phys. Rev. Lett. **73** 3544 (1994).
[8] B. J. Duda *et al.*, Phys. Rev. Lett. **83**, 1978 (1999); B. J. Duda and W. B. Mori, Phys. Rev E **61**, 1925 (2000).
[9] D. Anderson and M. Bonnedal, Phys. Fluids **22**, 105 (1979); D. Anderson and M. Lisak, Phys. Rev A **32**, 2270 (1985).
[10] A. V. Buryak *et al.*, Phys. Rev. Lett. **82**, 81 (1999).
[11] R. G. Hemker, PhD thesis, UCLA (2000); R. G. Hemker *et al.*, Proc. of the 1999 Particle Accelerator Conference, New York, 3672 (1999).

[12] C. J. McKinstrie and R. Bingham, Phys. Fluids B **1**, 230 (1989).
[13] C. J. McKinstrie and D. A. Russell, Phys. Rev. Lett. **61**, 2929 (1988).
[14] E. Esarey *et al.*, Appl. Phys. Lett. **53**, 1266 (1988).
[15] A. Pukhov and J. Meyer-ter-Vehn, Phys. Rev. Lett. **76**, 3975 (1996).
[16] K.-C. Tzeng and W. B. Mori, Phys. Rev. Lett. **81**, 104 (1998) and the references therein.

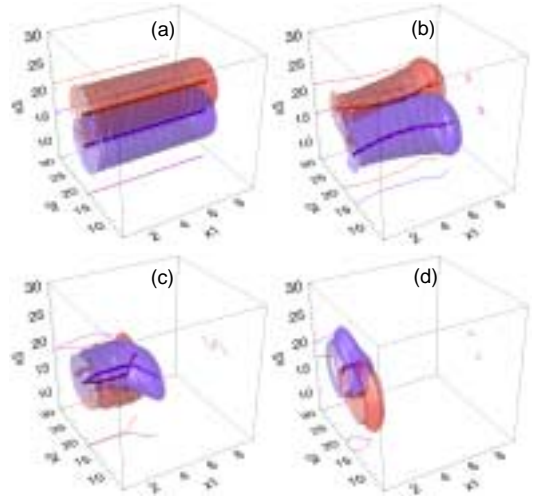


FIG. 1. (color). A time sequence of iso-surfaces of $E_j^2 = 5$ and the calculated centroids for each laser where $L = \Omega d_0$. The lines on the box walls are projections of the centroids. The length is in c/ω_p and the respective times are: (a) $t = 0$, (b) $t = 180/\omega_p$, (c) $t = 360/\omega_p$ and (d) $t = 540/\omega_p$.

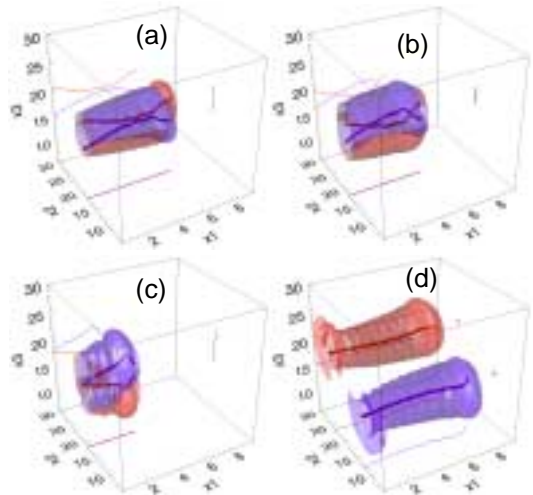


FIG. 2. (color). Iso-surfaces ($E_j^2 = 5$) and centroids for each laser for two cases. Fig. (a)-(c) corresponds to a time sequence of (a) $t = 240/\omega_p$, (b) $t = 300/\omega_p$ and (c) $t = 420/\omega_p$ for a case where $L = 0$. Fig. (d) corresponds to a case with $L = 1.7\Omega d_0$ at $t = 240/\omega_p$. The initial configurations of both cases are identical as Fig. 1(a).